Diagnosis, Assessment & Disease Monitoring

Exploratory correlation of the human structural connectome with non-MRI variables in Alzheimer's disease

Iman Aganj[1,2] 🄳 | **Jocelyn Mora**[1] | **Aina Frau-Pascual**[1,2] | **Bruce Fischl**[1,2] | for the Alzheimer's Disease Neuroimaging Initiative

[1]Athinoula A. Martinos Center for Biomedical Imaging, Radiology Department, Massachusetts General Hospital, Boston, Massachusetts, USA

[2]Radiology Department, Harvard Medical School, Boston, Massachusetts, USA

Correspondence
Iman Aganj, 149, 13th St., Suite 2301, Boston, MA 02129, USA.
Email: iaganj@mgh.harvard.edu

Abstract

Introduction: Discovery of the associations between brain structural connectivity and clinical and demographic variables can help to better understand the vulnerability and resilience of the brain architecture to neurodegenerative diseases and to discover biomarkers.

Methods: We used four diffusion-MRI databases, three related to Alzheimer's disease (AD), to exploratorily correlate structural connections between 85 brain regions with non-MRI variables, while stringently correcting the significance values for multiple testing and ruling out spurious correlations via careful visual inspection. We repeated the analysis with brain connectivity augmented with multi-synaptic neural pathways.

Results: We found 85 and 101 significant relationships with direct and augmented connectivity, respectively, which were generally stronger for the latter. Age was consistently linked to decreased connectivity, and healthier clinical scores were generally linked to increased connectivity.

Discussion: Our findings help to elucidate which structural brain networks are affected in AD and aging and highlight the importance of including indirect connections.

KEYWORDS
aging, Alzheimer's disease, dementia, diffusion MRI, human connectome, multi-synaptic neural pathways, structural brain connectivity

1 | INTRODUCTION

Normal aging, as well as debilitating neurodegenerative diseases such as Alzheimer's disease (AD), affect not only individual brain regions, but also the connectivity between them.[1,2] A focus on brain regions, but not interregional connectivity, may have hindered progress in understanding and treating diseases such as AD that are characterized as disconnection syndromes.[3] Mapping the complex brain networks through which information flows—that is, the human connectome[4]—can help to better understand the vulnerability and resilience of these networks to the effects of AD, potentially leading to the discovery of diagnostically and therapeutically important connectomic biomarkers. Analysis of structural brain networks, by means of noninvasive diffusion-weighted magnetic resonance imaging (dMRI), has proved valuable in revealing the structural basis of dysfunction in mild cognitive impairment (MCI) and AD, demonstrating changes distinct from those with healthy aging.[5-9]

Brain connectivity is often represented as a graph adjacency matrix of connection strengths between the brain regions of interest (ROIs), with its number of elements (graph edges) growing quadratically with respect to the number of ROIs (graph nodes). In population connectomic studies, it is often desired to find links between brain connectivity and non-MRI (clinical and/or demographic) variables. Such a study typically has sufficient statistical power to test pre-hypothesized relationships involving specific brain connections and variables. In contrast, an exploratory investigation to discover previously unknown relationships would require correlating the connectivity strength of every brain ROI pair with every available variable, amounting to hundreds of thousands (sometimes millions) of tests. In that scenario, the correction for multiple comparisons would make the study statistically less powerful and consequently less desirable to conduct. Alternatively, one could reduce the number of tests considerably by focusing on network summary features[10] rather than brain connections, which would inform about how the variables relate to the network as a whole[7,11] but not to individual brain connections.

Structural connectivity between two brain regions is commonly defined based on the dMRI tractography-derived[12,13] streamlines between them. The direct fiber bundle connecting two brain areas is expected to be the major signal carrier between them; however, multi-synaptic neural pathways (those mediated through other regions) also provide connectivity.[14,15] We have previously developed computational methods to augment direct structural connectivity graphs with indirect connections[16] as well as quantify brain structural connectivity while accounting for indirect pathways,[17] and have shown the importance of these pathways in predicting functional connectivity [17] and deriving connectomic biomarkers for MCI and AD.[18]

Here, we take an exploratory approach to discovering relationships that individual structural connections in the brain may have with clinical and demographic variables. We use anatomical and diffusion MR images along with non-MRI data from four public databases (three of which are related to AD) to find links between brain connections—both direct and augmented—and non-MRI variables that remain significant after stringent correction for multiple testing and visual inspection.

RESEARCH IN CONTEXT

1. **Systematic review**: The literature was reviewed in Google Scholar. Most structural connectomic analyses of Alzheimer's disease (AD) examined network features, predefined fiber tracts, and/or pre-hypothesized non-MRI variables, thereby falling short of being an exhaustive exploratory analysis. They also almost exclusively studied direct structural connections.

2. **Interpretation**: Consistent with prior literature, the significant relationships that we found showed increased brain structural connectivity with healthier clinical scores, youth, and retention rate. The relationships with augmented (direct + indirect) connectivity were generally stronger than—but not totally overlapping with—those with direct connectivity.

3. **Future directions**: The significant relationships between brain connectivity and non-MRI variables that were found in this exploratory study can be hypothesized and directly tested in additional databases and/or with different connectivity quantification techniques in the future, thereby validated (or falsified) through replication. The generated knowledge will help to define the specific brain networks that are affected in AD.

We describe our processing and analysis methods in Section 2, report our results in Section 3, discuss them in Section 4, and conclude the paper in Section 5.

2 | METHODS

2.1 | Datasets

We used the following four public dMRI databases. The number of subjects indicates the subset of subjects that were processed and included in our analysis, and the number of non-MRI variables indicates variables that were available for at least some of the included subjects.

- The second phase of the Alzheimer's Disease Neuroimaging Initiative (ADNI-2)[19]: 217 subjects (from cognitively normal to AD), 47 non-MRI variables from the ADNIMERGE table (demographics, cerebrospinal fluid [CSF] markers, dementia/cognitive exam scores, positron emission tomography [PET], apolipoprotein E4 [*APOE4*], diagnosis, etc.).
- The third release in the Open Access Series of Imaging Studies (OASIS-3)[20]: 771 subjects (from cognitively normal to AD), 588 non-MRI variables (demographics, Uniform Data Set, dementia/cognitive exam scores, *APOE*, etc.).

- The Pre-symptomatic Evaluation of Experimental or Novel Treatments for Alzheimer's Disease (PREVENT-AD)[21]: 340 cognitively unimpaired older individuals with a parental or multiple-sibling history of AD, 199 non-MRI variables (demographics, medical history, vitals, CSF markers, dementia/cognitive exam subscores, genetics, lab results, auditory/olfactory processing, etc.).
- The WashU-UMN Human Connectome Project (HCP)[22]: 617 healthy young adults, 488 non-MRI variables (demographics, medical history, family history, dementia/cognitive exam scores, personality/emotion tests, motor/sensory tests, task performance, etc.).

2.2 | Data processing

Anatomical MR images of the databases were processed with FreeSurfer.[23] All time points of PREVENT-AD were also more robustly processed using the FreeSurfer longitudinal pipeline.[24] For all databases, we included each subject only once, that is, the earliest visit containing dMRI (frequently the baseline), in order to keep our analyzed data points independent and our study cross-sectional. We then ran the FreeSurfer dMRI processing pipeline, which also includes commands from the FMRIB Software Library (FSL),[25] and propagated 85 automatically segmented cortical and subcortical regions from the structural to the diffusion space using boundary-based image registration.[26]

Next, we used our public toolbox (www.nitrc.org/projects/csaodf-hough) to (1) reconstruct the diffusion orientation distribution function in constant solid angle (CSA-ODF),[27] (2) run Hough-transform global probabilistic tractography[13] to generate an optimal (highest-score) streamline passing through each of the 10,000 seed points per subject, (3) compute a symmetric structural connectivity matrix (with positive elements) for each subject by summing the tracts passing through each pair of ROIs weighted by the tract score (hence an emphasis on streamlines best aligned with the dMRI-derived fiber orientations as well as fiber tracts with the highest white-matter integrity), and (4) augment the raw matrices with indirect connections (see Section 2.3).[16] We transformed the connectivity value c (each element in the raw or augmented connectivity matrix) as $c \leftarrow 1 - \exp(-c/\bar{c})$, where $\bar{c}$ is the cross-subject average of c, thereby confining the connectivity values to the range [0,1].

2.3 | Augmentation of structural connectivity with indirect connections

Strong functional connectivity between brain regions is commonly observed between regions with no *direct* structural connection.[14,28–34] Some variance in functional connectivity unexplained by direct connections can be accounted for rather by *indirect* structural connections,[14,15,17] implying that the network nature of the brain makes the interaction between two brain areas sensitive to influences from other remote areas.[29]

We have previously developed a method to augment a tractography-generated structural connectivity matrix with indirect connections via the mathematics of circuit laws,[16] thereby producing a new matrix that additionally reflects multi-synaptic pathways. This approach is based on the intuition that total connectivity for multiple direct connections is expectedly their sum if they are parallel, or smaller than each connection if they are in series (as total connectivity is presumably bottlenecked by the weakest link along the way). These conditions are accommodated by modeling the brain similarly to a resistive electrical circuit, where a resistor represents each direct connection, with its conductance (inverse of resistance) being the tractography-measured strength of the connection.[16,35] Total (augmented) connectivity is then calculated via Kirchhoff's laws as the overall conductance among regions, using graph Laplacian methods.

2.4 | Analysis

We used the cross-sectional data of each database to independently test if there is a statistically significant relationship between each non-MRI (clinical or demographic) variable and the computed structural brain connection between each ROI pair. To perform a true exploratory analysis, we did not exclude any available variable based on its perceived relevance. To deal with data source heterogeneity, we analyzed the databases (and report their results) separately. The homogeneity within each database is expected to lead to findings that would be strengthened if they independently replicated in several databases.

If a non-MRI variable had categorical (rather than numeric) values, we converted it to numeric by assigning a natural number to each category, while making our best effort to sort the categories (if more than two) in a monotonic order; for instance, for the variable "Baseline Diagnosis" in ADNI-2, we assigned the following: Control Normal → (1), Significant Memory Concern → (2), Early MCI → (3), Late MCI → (4), and AD → (5). We computed the Pearson correlation coefficient (r), along with its significance (p) value, between each variable and each connection. The p-values were then corrected for multiple comparisons via the conservative Bonferroni method (p_b); that is, they were multiplied by the number of (undirected) connections, #ROIs × (#ROIs − 1) ÷ 2 = 85 × 84 ÷ 2 = 3570, as well as by the number of studied variables (see Section 2.1). Since the quantified structural connectivity, which is the score-weighted number of streamlines passing through a pair of ROIs, is affected by the tract length, we controlled for the extraneous variable of intracranial volume (ICV) by computing the partial correlation instead. For robustness of the correlation,[36] we removed connectivity values that were marginal outliers from the correlation analysis by excluding any element in the connectivity matrix of a subject (but not the subject's entire matrix) that was larger than 0.9 (recall the range [0,1] of values). This was principally because we deemed a connectivity value with a large deviation from the population mean to be less reliable, since such a deviation indicated an increased likelihood of lower image quality or a data-processing issue. Therefore, slightly different numbers of subjects contributed to the correlation analysis of different brain connections.

For each variable, we selected the connection most significantly correlating with it, that is, with the lowest p_b-value. If p_b was smaller than the threshold $\alpha = 0.05$, then we scatter-plotted the connection strength with respect to the variable and visually inspected it to ensure the significant Pearson correlation was real and not spurious due to some outliers, thus avoiding situations with most data points clustered together with no obvious relationship.[36] The correlations surviving the Bonferroni correction and passing the visual inspection are reported as follows.

3 | RESULTS

Cross-subject medians of the raw and augmented connectivity matrices are shown in Figure 1 for the four databases. We correlated 3570 brain structural connections with 47, 588, 199, and 488 non-MRI variables for the ADNI-2, OASIS-3, PREVENT-AD, and HCP databases, respectively, while controlling for the ICV. Out of those variables, 15, 230, 32, and 84, respectively, were found to have a significant Pearson correlation ($p_b < 0.05$) with raw connections, and 20, 79, 1, and 1 variables, respectively, had a significant correlation with augmented connections. After visual inspection to remove spurious correlations, variables with significant correlation with raw connectivity were reduced to 15, 65, 3, and 2, respectively, whereas the variables significantly correlated with augmented connectivity remained unchanged. The findings are detailed in Tables 1-4 for the four databases. The right column of each table indicates the total number (out of 3570) of connections reaching Bonferroni-level significance for a given variable.

Controlling for ICV had several effects on the results; for example, it made the correlation of brain connectivity with the variable Everyday Cognition Study Partner Report–Memory in ADNI-2 and with the Multilingual Naming Test (both the total score and the total correct without semantic cue) in OASIS-3 significant (see Tables 1 and 2). Without separating the effects of ICV, conversely, we would observe significant correlations of brain connectivity with grip strength (−) and the maximum number of drinks consumed in a single day (−) in HCP, and with posture issues (−) and with Montreal Cognitive Assessment: Abstraction (+) in OASIS-3. The confounding effect of ICV was especially drastic on the correlation with sex. Significant correlation of connectivity (of the most related brain connection) with the male sex was as follows:

- initially not found in ADNI-2 but appeared as positive by including ICV as a covariate,
- negative in OASIS-3 regardless of controlling for ICV (but stronger without),
- initially positive in PREVENT-AD but disappeared after including ICV as a covariate,
- negative in HCP regardless of controlling for ICV (but stronger without).

Next, we focused on three representative variables of age, the Mini-Mental State Examination (MMSE), and the Clinical Dementia Rating (CDR; sum of boxes). Among all the augmented brain connections that were significantly correlated with age (after Bonferroni correction) consistently in ADNI-2, OASIS-3, and PREVENT-AD, the one between the right superior frontal cortex and the left hippocampus was most significant (in terms of the geometric mean of the p-values across databases). Similarly, for both the MMSE and CDR, the augmented connection between the right superior frontal cortex and the right hippocampus had the most significant correlation consistently in ADNI-2 and OASIS-3. These relationships are plotted in Figure 2 for all three variables.

4 | DISCUSSION

Although more correlations were initially found to be significant with raw than augmented structural connectivity (in three out of four databases), visual inspection of the data led to discarding many of the former—but none of the latter—as spurious, implying more robustness and reliability of the augmented structural connections. Spuriousness was often because raw (direct) connectivity between an ROI pair was zero for all except a few subjects who dramatically influenced the correlation calculation, in contrast to augmented connectivity, which is always positive in a network with a single connected component. Eventually, a total of 85 relationships with raw connectivity and 101 with augmented connectivity passed the Pearson correlation threshold, Bonferroni correction, and visual inspection. Each variable may have been significantly correlated with multiple brain connections, the number of which is listed in the tables (right column). Out of 76 variables correlated with both types of connectivity (see the taller cells in the left column of the tables), 72 were more significantly correlated with augmented than raw connectivity, always with a greater or equal number of total connections correlated with augmented than raw connectivity. For a significance plot of the correlation with age, MMSE, and CDR for all connections (albeit in a non-exploratory context and with a different connectivity quantification method), see our previous report.[18]

More variables were found to be significantly related to brain connectivity in ADNI-2 and OASIS-3 (Tables 1 and 2) than in PREVENT-AD and HCP (Tables 3 and 4), possibly due to the fact that PREVENT-AD and HCP (which include only healthy subjects) are more homogenous populations with narrower ranges of scores (e.g. MMSE) than ADNI-2 and OASIS-3 (which include a mix of healthy, MCI, and AD subjects). Moreover, the fact that proxies for disease severity, such as MMSE and CDR, correlate with brain connectivity (only with the presence of MCI and AD patients) suggests that the corresponding changes in the connectome are possibly disease-related and a potential marker of the disease.

The most prominent non-MRI variable that was consistently correlated with structural connectivity was age. A negative correlation was observed between age and hippocampal connectivity in all databases except HCP. The limited age range in the young population of HCP may be the reason why this relationship was not detected in this database, given that the standard deviations of age were (in decreas-

FIGURE 1 Element-wise cross-subject median of the raw (left) and augmented (right) connectivity matrices for the four databases. ADNI-2, Alzheimer's Disease Neuroimaging Initiative; HCP, Human Connectome Project; OASIS-3, Open Access Series of Imaging Studies; PREVENT-AD, Pre-symptomatic Evaluation of Experimental or Novel Treatments for Alzheimer's Disease.

TABLE 1 Significant correlations of non-MRI variables with brain connectivity in ADNI-2.

Non-MRI variable	Most correlated brain structural connection (type [raw/augmented], Pearson correlation, Bonferroni-corrected p-value)	# Sig.Conn
Baseline diagnosis	L. Lingual cortex—L. Entorhinal cortex Augmented, $r = -0.41$, $p_b = 0.0005$	79
Age	L. Hippocampus—L. Ventral diencephalon Raw, $r = -0.42$, $p_b = 0.0002$	7
	L. Hippocampus—R. Superior frontal cortex Augmented, $r = -0.47$, $p_b = 7 \times 10^{-7}$	67
Sex	R. Putamen—Brainstem Raw, $r = 0.36$ (with the male sex), $p_b = 0.04$	2
FDG-PET Mean of angular, temporal, and posterior cingulate	R. Hippocampus—R. Fusiform cortex Raw, $r = 0.43$, $p_b = 0.0001$	3
	R. Hippocampus—R. Precuneus cortex Augmented, $r = 0.46$, $p_b = 4 \times 10^{-6}$	67
AV45 PET (binding to β-amyloid) Mean of whole cerebellum	R. Hippocampus—R. Precuneus cortex Augmented, $r = -0.43$, $p_b = 8 \times 10^{-5}$	45
Clinical Dementia Rating (CDR) Sum of boxes	R. Hippocampus—R. Fusiform cortex Raw, $r = -0.38$, $p_b = 0.007$	3
	R. Entorhinal cortex—L. Pallidum Augmented, $r = -0.43$, $p_b = 6 \times 10^{-5}$	135
AD Assessment Scale (ADAS) 11 items	R. Hippocampus—R. Fusiform cortex *Raw*, $r = -0.37$, $p_b = 0.03$	2
	R. Hippocampus—R. Precuneus cortex Augmented, $r = -0.43$, $p_b = 0.0001$	45
AD Assessment Scale (ADAS) 13 items	R. Hippocampus—R. Fusiform cortex Raw, $r = -0.39$, $p_b = 0.005$	2
	R. Hippocampus—R. Precuneus cortex Augmented, $r = -0.44$, $p_b = 4 \times 10^{-5}$	86
AD Assessment Scale (ADAS) Delayed Word Recall	R. Hippocampus—R. Ventral diencephalon Raw, $r = -0.38$, $p_b = 0.01$	4
	L. Entorhinal cortex—R. Caudal anterior cingulate cortex Augmented, $r = -0.40$, $p_b = 0.0008$	42
Mini-mental state examination (MMSE)	R. Hippocampus—R. Entorhinal cortex Raw, $r = 0.37$, $p_b = 0.02$	2
	L. Amygdala—R. Entorhinal cortex Augmented, $r = 0.42$, $p_b = 0.0003$	75
Rey Auditory Verbal Learning Test (RAVLT) Immediate Sum of 5 trials	R. Hippocampus—R. Entorhinal cortex Raw, $r = 0.39$, $p_b = 0.006$	1
	R. Isthmus cingulate cortex—L. Entorhinal cortex Augmented, $r = 0.41$, $p_b = 0.0005$	70
Functional assessment questionnaire (FAQ)	R. Hippocampus—R. Fusiform cortex Raw, $r = -0.38$, $p_b = 0.01$	2
	R. Hippocampus—R. Rostral middle frontal cortex Augmented, $r = -0.46$, $p_b = 10^{-6}$	142
Montreal cognitive assessment (MoCA)	L. Hippocampus—L. Middle temporal cortex Raw, $r = 0.39$, $p_b = 0.01$	2

(Continues)

TABLE 1 (Continued)

Non-MRI variable	Most correlated brain structural connection (type [raw/augmented], Pearson correlation, Bonferroni-corrected p-value)	# Sig.Conn
	R. Hippocampus—R. Isthmus cingulate cortex Augmented, $r = 0.44$, $p_b = 6 \times 10^{-5}$	71
ADNI modified Preclinical Alzheimer's Cognitive Composite (PACC) with Digit Symbol Substitution	R. Hippocampus—R. Entorhinal cortex Raw, $r = 0.40$, $p_b = 0.001$	6
	R. Hippocampus—L. Rostral middle frontal cortex Augmented, $r = 0.44$, $p_b = 2 \times 10^{-5}$	161
ADNI modified Preclinical Alzheimer's Cognitive Composite (PACC) with Trails B	R. Parahippocampal cortex—R. Fusiform cortex Raw, $r = 0.41$, $p_b = 0.0005$	6
	R. Hippocampus—L. Rostral middle frontal cortex Augmented, $r = 0.44$, $p_b = 10^{-5}$	173
Everyday Cognition Study Partner Report (ECog SP)—Memory	L. Entorhinal cortex—L. Banks of superior temporal sulcus Augmented, $r = -0.37$, $p_b = 0.02$	1
Everyday Cognition Study Partner Report (ECog SP)—Language	L. Isthmus cingulate cortex—L. Middle temporal cortex Augmented, $r = -0.38$, $p_b = 0.01$	4
Everyday Cognition Study Partner Report (ECog SP)—Plan	R. Isthmus cingulate cortex—L. Inferior temporal cortex Augmented, $r = -0.39$, $p_b = 0.009$	2
Everyday Cognition Study Partner Report (ECog SP)—Total	L. Hippocampus—L. Entorhinal cortex Raw, $r = -0.37$, $p_b = 0.04$	1
	R. Isthmus cingulate cortex—L. Inferior temporal cortex Augmented, $r = -0.39$, $p_b = 0.006$	4
Logical Memory Delayed Recall	R. Hippocampus—L. Rostral middle frontal cortex Augmented, $r = 0.37$, $p_b = 0.01$	6
Trail Making Test, Part B Time to complete	R. Parahippocampal cortex—R. Fusiform cortex Raw, $r = -0.40$, $p_b = 0.001$	1
	R. Hippocampus—R. Isthmus cingulate cortex Augmented, $r = -0.37$, $p_b = 0.04$	1

Abbreviation: ADNI-2, Alzheimer's Disease Neuroimaging Initiative; AV45, florbetapir; FDG, fludeoxyglucose-18; MRI, magnetic resonance imaging; PET, positron emission tomography; # Sig.Conn, number of significantly correlated connect.

ing order) 9.1 years in OASIS-3, 6.9 years in ADNI-2, 5.1 years in PREVENT-AD, but only 3.6 years in HCP. In fact, the statistical significance of the age correlation decreased in the same database order.

Clinical scores that were found to be significantly related to brain connectivity showed the consistent trend of healthier scores being linked to increased connectivity. The only exception was the significant relationship of phosphorylated tau with the raw connection between the right caudate and the left caudal middle frontal cortex in PREVENT-AD, which was unanticipatedly positive. Nonetheless, we had already observed—in a different database with a different connectivity quantification method—a similarly unexpected strengthening of caudal structural connectivity with worsening cognitive status.[18,37] In fact, volume[38] and fractional anisotropy (FA)[39] of the caudate have been reported to increase in presymptomatic familial AD, which might have also led to the aforementioned relationship we observed in PREVENT-

AD (which includes healthy subjects at risk of AD). Such an increase in the measured structural connectivity in presymptomatic subjects may indicate a compensatory effect,[40] or could stem from other factors (eg, selective axonal loss can increase FA in regions with fiber crossing[39,41,42]).

The number of imaging sessions and clinical data available for a subject in OASIS-3 were positively related to (mostly) hippocampal connectivity. This could be attributable to a higher follow-up rate for those with healthier hippocampi, as individuals with MCI and dementia have been shown to have lower retention rates in research studies than those with normal cognition.[43,44]

With larger ICV, brain regions become farther apart from each other, thus harder to reach by streamline tractography. Therefore, we decided to control for ICV in our regression analysis to avoid underestimation of brain connectivity. Doing so eliminated (in some databases) correlation of brain connectivity with several variables,

TABLE 2 Significant correlations of non-MRI variables with brain connectivity in OASIS-3.

Non-MRI variable	Most correlated brain structural connection (type [raw/augmented], Pearson correlation, Bonferroni-corrected p-value)	# Sig. Conn
Age	L. Hippocampus—L. Thalamus Raw, $r = -0.48$, $p_b = 9 \times 10^{-35}$	266
	L. Hippocampus—R. Lingual cortex Augmented, $r = -0.5$, $p_b = 3 \times 10^{-41}$	2232
Sex	R. Thalamus—L. Thalamus Raw, $r = -0.21$ (with the male sex), $p_b = 0.04$	1
Uniform data set (UDS) Number of available sessions	L. Superior parietal cortex—L. Precuneus cortex Raw, $r = 0.37$, $p_b = 5 \times 10^{-18}$	73
	R. Inferior parietal cortex—L. Inferior parietal cortex Augmented, $r = 0.34$, $p_b = 3 \times 10^{-13}$	1430
Neuropsychological assessment Number of available sessions	L. Superior parietal cortex—L. Precuneus cortex Raw, $r = 0.38$, $p_b = 9 \times 10^{-13}$	105
	L. Pericalcarine cortex—L. Parahippocampal cortex Augmented, $r = 0.41$, $p_b = 10^{-16}$	2519
ADRC clinical data Number of available sessions	L. Superior parietal cortex—L. Precuneus cortex Raw, $r = 0.31$, $p_b = 4 \times 10^{-11}$	58
	R. Inferior parietal cortex—R. Fusiform cortex Augmented, $r = 0.31$, $p_b = 2 \times 10^{-11}$	1060
Number of PET sessions	R. Hippocampus—R. Fusiform cortex Raw, $r = 0.3$, $p_b = 4 \times 10^{-7}$	19
	L. Hippocampus—R. Cuneus cortex Augmented, $r = 0.34$, $p_b = 7 \times 10^{-11}$	574
Number of MRI sessions	R. Hippocampus—R. Middle temporal cortex Raw, $r = 0.35$, $p_b = 3 \times 10^{-15}$	74
	R. Hippocampus—R. Precuneus cortex Augmented, $r = 0.38$, $p_b = 10^{-20}$	1937
Number of CT sessions	R. Hippocampus—R. Superior frontal cortex Augmented, $r = 0.25$, $p_b = 0.01$	1
Presumed disease status at enrollment (higher is healthier)	R. Hippocampus—R. Ventral diencephalon Raw, $r = 0.25$, $p_b = 0.0004$	10
	R. Hippocampus—L. Superior frontal cortex Augmented, $r = 0.3$, $p_b = 7 \times 10^{-10}$	336
Level of independence (higher is more dependent)	R. Hippocampus—L. Hippocampus Augmented, $r = -0.29$, $p_b = 4 \times 10^{-8}$	182
Form A3 has been submitted previously and there have been no changes.	R. Precuneus cortex—L. Precuneus cortex Raw, $r = -0.31$, $p_b = 5 \times 10^{-7}$	39
	R. Rostral anterior cingulate cortex—L. Temporal pole cortex Augmented, $r = -0.37$, $p_b = 10^{-12}$	1822
Mother living	L. Hippocampus—R. Superior frontal cortex Augmented, $r = 0.25$, $p_b = 0.001$	8
Father living	R. Thalamus—L. Isthmus cingulate cortex Raw, $r = 0.26$, $p_b = 0.0007$	2
Sibling 1 living	R. Hippocampus—R. Fusiform cortex Raw, $r = 0.24$, $p_b = 0.02$	1
	R. Hippocampus—R. Superior frontal cortex Augmented, $r = 0.25$, $p_b = 0.006$	10
Sibling 2 living	R. Hippocampus—R. Fusiform cortex Raw, $r = 0.28$, $p_b = 0.04$	1
Subject wearing a hearing aid	L. Lingual cortex—L. Putamen Raw, $r = -0.21$, $p_b = 0.02$	1

(Continues)

TABLE 2 (Continued)

Non-MRI variable	Most correlated brain structural connection (type [raw/augmented], Pearson correlation, Bonferroni-corrected *p*-value)	# Sig. Conn
	R. Lingual cortex—L. Pallidum Augmented, $r = -0.22$, $p_b = 0.006$	10
History or presence of hypertension	R. Superior frontal cortex—R. Thalamus Augmented, $r = -0.23$, $p_b = 0.001$	14
Hachinski Ischemic score	R. Superior frontal cortex—R. Ventral diencephalon Raw, $r = -0.22$, $p_b = 0.03$	1
	R. Superior frontal cortex—R. Thalamus Augmented, $r = -0.25$, $p_b = 9 \times 10^{-5}$	20
Mini-mental state examination (MMSE)	R. Hippocampus—R. Putamen Raw, $r = 0.29$, $p_b = 7 \times 10^{-9}$	40
	R. Hippocampus—L. Precentral cortex Augmented, $r = 0.38$, $p_b = 3 \times 10^{-20}$	702
CDR memory	R. Hippocampus—R. Amygdala Raw, $r = -0.33$, $p_b = 3 \times 10^{-13}$	65
	R. Hippocampus—L. Thalamus Augmented, $r = -0.41$, $p_b = 7 \times 10^{-25}$	1499
CDR orientation	R. Hippocampus—R. Amygdala Raw, $r = -0.3$, $p_b = 10^{-9}$	37
	R. Hippocampus—L. Insula cortex Augmented, $r = -0.37$, $p_b = 2 \times 10^{-18}$	1080
CDR Judgment and problem-solving	R. Hippocampus—R. Amygdala Raw, $r = -0.31$, $p_b = 2 \times 10^{-10}$	48
	R. Hippocampus—R. Superior frontal cortex Augmented, $r = -0.39$, $p_b = 3 \times 10^{-21}$	993
CDR Community affairs	R. Hippocampus—R. Superior frontal cortex Augmented, $r = -0.35$, $p_b = 2 \times 10^{-16}$	594
CDR Home and hobbies	R. Hippocampus—R. Amygdala Raw, $r = -0.29$, $p_b = 7 \times 10^{-9}$	38
	R. Hippocampus—L. Thalamus Augmented, $r = -0.38$, $p_b = 10^{-20}$	938
CDR Sum of boxes	R. Hippocampus—R. Amygdala Raw, $r = -0.32$, $p_b = 10^{-11}$	46
	R. Hippocampus—L. Thalamus Augmented, $r = -0.4$, $p_b = 2 \times 10^{-23}$	1199
CDR Total score	R. Hippocampus—R. Amygdala Raw, $r = -0.33$, $p_b = 10^{-12}$	55
	R. Hippocampus—L. Thalamus Augmented, $r = -0.41$, $p_b = 10^{-24}$	1163
Difficulty or needing help with paying bills	R. Hippocampus—R. Amygdala Raw, $r = -0.27$, $p_b = 2 \times 10^{-6}$	19
	R. Hippocampus—R. Superior frontal cortex Augmented, $r = -0.33$, $p_b = 2 \times 10^{-12}$	579
Difficulty or needing help with taxes and business affairs	R. Hippocampus—R. Amygdala Raw, $r = -0.27$, $p_b = 10^{-6}$	23
	R. Hippocampus—L. Thalamus Augmented, $r = -0.34$, $p_b = 5 \times 10^{-14}$	535
Difficulty or needing help with shopping alone	R. Hippocampus—R. Ventral diencephalon Raw, $r = -0.25$, $p_b = 0.0004$	4
	R. Hippocampus—L. Thalamus Augmented, $r = -0.3$, $p_b = 10^{-9}$	225

(Continues)

TABLE 2 (Continued)

Non-MRI variable	Most correlated brain structural connection (type [raw/augmented], Pearson correlation, Bonferroni-corrected p-value)	# Sig. Conn
Difficulty or needing help with games and hobbies	L. Hippocampus—L. Ventral diencephalon Raw, $r = -0.22$, $p_b = 0.03$	1
	L. Hippocampus—R. Hippocampus Augmented, $r = -0.28$, $p_b = 2 \times 10^{-7}$	97
Difficulty or needing help with preparing a balanced meal	R. Hippocampus—R. Amygdala Raw, $r = -0.23$, $p_b = 0.003$	4
	R. Hippocampus—L. Pallidum Augmented, $r = -0.3$, $p_b = 10^{-9}$	213
Difficulty or needing help with keeping track of current events	R. Hippocampus—R. Ventral diencephalon Raw, $r = -0.23$, $p_b = 0.01$	1
	R. Hippocampus—L. Thalamus Augmented, $r = -0.28$, $p_b = 3 \times 10^{-8}$	112
Difficulty or needing help with paying attention	R. Hippocampus—R. Fusiform cortex Raw, $r = -0.23$, $p_b = 0.002$	2
	R. Hippocampus—L. Precuneus cortex Augmented, $r = -0.29$, $p_b = 5 \times 10^{-9}$	369
Difficulty or needing help with remembering dates	R. Hippocampus—R. Ventral diencephalon Raw, $r = -0.24$, $p_b = 0.001$	2
	R. Hippocampus—L. Insula cortex Augmented, $r = -0.29$, $p_b = 5 \times 10^{-9}$	106
Difficulty or needing help with traveling and driving	R. Hippocampus—R. Ventral diencephalon Raw, $r = -0.29$, $p_b = 10^{-7}$	24
	R. Hippocampus—R. Superior frontal cortex Augmented, $r = -0.35$, $p_b = 6 \times 10^{-16}$	452
Decline reported by subject	L. Thalamus—L. Parahippocampal cortex Raw, $r = -0.22$, $p_b = 0.02$	4
	L. Hippocampus—R. Superior frontal cortex Augmented, $r = -0.29$, $p_b = 6 \times 10^{-9}$	292
Decline reported by informant	R. Hippocampus—R. Amygdala Raw, $r = -0.28$, $p_b = 10^{-7}$	40
	L. Hippocampus—R. Superior frontal cortex Augmented, $r = -0.39$, $p_b = 3 \times 10^{-20}$	1341
Decline reported by clinician	R. Hippocampus—R. Fusiform cortex Raw, $r = -0.32$, $p_b = 10^{-10}$	66
	R. Hippocampus—R. Superior frontal cortex Augmented, $r = -0.43$, $p_b = 10^{-24}$	1611
Cognitive impairment reported by clinician	R. Hippocampus—R. Fusiform cortex Raw, $r = -0.28$, $p_b = 0.0001$	18
	L. Hippocampus—R. Lingual cortex Augmented, $r = -0.36$, $p_b = 6 \times 10^{-11}$	223
WAIS Information	R. Hippocampus—R. Inferior temporal cortex Raw, $r = 0.26$, $p_b = 0.001$	9
	R. Hippocampus—L. Caudate Augmented, $r = 0.35$, $p_b = 10^{-11}$	344
WAIS block design	R. Hippocampus—R. Fusiform cortex Raw, $r = 0.36$, $p_b = 2 \times 10^{-12}$	54
	R. Hippocampus—L. Precentral cortex Augmented, $r = 0.4$, $p_b = 4 \times 10^{-17}$	1505
WAIS WAIS-R digit symbol	L. Hippocampus—L. Fusiform cortex Raw, $r = 0.39$, $p_b = 3 \times 10^{-15}$	96

(Continues)

TABLE 2 (Continued)

Non-MRI variable	Most correlated brain structural connection (type [raw/augmented], Pearson correlation, Bonferroni-corrected p-value)	# Sig. Conn
	L. Hippocampus—R. Superior frontal cortex Augmented, $r = 0.45$, $p_b = 5 \times 10^{-24}$	1541
WMS Associate learning summary score	L. Hippocampus—L. Thalamus Raw, $r = 0.31$, $p_b = 10^{-8}$	41
	L. Hippocampus—R. Superior frontal cortex Augmented, $r = 0.38$, $p_b = 3 \times 10^{-17}$	691
WMS Digit Span Backward	L. Hippocampus—L. Thalamus Raw, $r = 0.25$, $p_b = 0.01$	1
	L. Hippocampus—L. Superior frontal cortex Augmented, $r = 0.27$, $p_b = 0.0005$	29
WMS WMS-III letter-number sequencing	L. Parahippocampal cortex—L. Ventral diencephalon Raw, $r = 0.26$, $p_b = 10^{-5}$	16
	R. Hippocampus—L. Superior frontal cortex Augmented, $r = 0.33$, $p_b = 10^{-12}$	255
Total animals named in 60 s	R. Hippocampus—R. Ventral diencephalon Raw, $r = 0.27$, $p_b = 3 \times 10^{-6}$	29
	R. Hippocampus—L. Superior frontal cortex Augmented, $r = 0.35$, $p_b = 8 \times 10^{-16}$	350
Total vegetables named in 60 s	L. Hippocampus—L. Inferior temporal cortex Raw, $r = 0.27$, $p_b = 5 \times 10^{-5}$	10
	R. Hippocampus—L. Precentral cortex Augmented, $r = 0.31$, $p_b = 6 \times 10^{-9}$	181
Mental control total score	L. Hippocampus—R. Superior frontal cortex Augmented, $r = 0.27$, $p_b = 0.0001$	72
Trail Making Test, Part A Time to complete	R. Hippocampus—R. Fusiform cortex Raw, $r = -0.29$, $p_b = 3 \times 10^{-8}$	35
	R. Hippocampus—L. Superior frontal cortex Augmented, $r = -0.37$, $p_b = 5 \times 10^{-18}$	836
Trail Making Test, Part B Time to complete	L. Hippocampus—L. Fusiform cortex Raw, $r = -0.34$, $p_b = 2 \times 10^{-13}$	94
	L. Hippocampus—R. Superior frontal cortex Augmented, $r = -0.43$, $p_b = 3 \times 10^{-26}$	1643
Boston Naming Test 60 items	R. Hippocampus—R. Inferior temporal cortex Raw, $r = 0.29$, $p_b = 2 \times 10^{-5}$	20
	R. Hippocampus—R. Thalamus Augmented, $r = 0.37$, $p_b = 2 \times 10^{-12}$	1142
Current logical memory IA story units recalled	R. Hippocampus—R. Amygdala Raw, $r = 0.3$, $p_b = 7 \times 10^{-6}$	13
	R. Hippocampus—L. Ventral diencephalon Augmented, $r = 0.36$, $p_b = 4 \times 10^{-11}$	478
Logical memory IIA—Delayed story units recalled	R. Hippocampus—R. Amygdala Raw, $r = 0.31$, $p_b = 5 \times 10^{-7}$	26
	R. Hippocampus—L. Ventral diencephalon Augmented, $r = 0.38$, $p_b = 3 \times 10^{-13}$	757
Simon percent correct	R. Hippocampus—L. Hippocampus Augmented, $r = 0.25$, $p_b = 0.0003$	36
Simon number of correct on all trials	L. Hippocampus—R. Superior frontal cortex Augmented, $r = 0.26$, $p_b = 4 \times 10^{-5}$	53
Switch pure CV number correct	L. Hippocampus—R. Superior parietal cortex Augmented, $r = 0.23$, $p_b = 0.006$	7

(Continues)

TABLE 2 (Continued)

Non-MRI variable	Most correlated brain structural connection (type [raw/augmented], Pearson correlation, Bonferroni-corrected p-value)	# Sig. Conn
Switch mixed number correct	L. Hippocampus—L. Ventral diencephalon Raw, $r = 0.26$, $p_b = 0.0002$	15
	L. Hippocampus—R. Caudate Augmented, $r = 0.34$, $p_b = 2 \times 10^{-11}$	205
Switch percent correct	L. Hippocampus—L. Fusiform cortex Raw, $r = 0.27$, $p_b = 2 \times 10^{-5}$	11
	L. Hippocampus—R. Precuneus cortex Augmented, $r = 0.34$, $p_b = 8 \times 10^{-13}$	338
Benson complex figure copy	R. Hippocampus—L. Inferior temporal cortex Augmented, $r = 0.26$, $p_b = 0.02$	3
Craft Story 21 recall (Immediate) verbatim scoring	R. Hippocampus—R. Superior frontal cortex Augmented, $r = 0.29$, $p_b = 0.0008$	6
Craft Story 21 recall (Immediate) paraphrase scoring	R. Hippocampus—R. Superior frontal cortex Augmented, $r = 0.32$, $p_b = 9 \times 10^{-6}$	42
Craft Story 21 recall (Delayed) verbatim scoring	R. Hippocampus—R. Superior frontal cortex Augmented, $r = 0.28$, $p_b = 0.003$	8
Craft Story 21 recall (Delayed) paraphrase scoring	R. Hippocampus—R. Superior frontal cortex Augmented, $r = 0.3$, $p_b = 0.0002$	26
MINT total score	R. Hippocampus—L. Caudate Augmented, $r = 0.28$, $p_b = 0.04$	1
MINT total correct without semantic cue	R. Hippocampus—L. Caudate Augmented, $r = 0.28$, $p_b = 0.04$	1
MINT phonemic cues: number given	R. Hippocampus—L. Caudate Augmented, $r = -0.3$, $p_b = 0.004$	4
MoCA Total Raw Score—uncorrected	R. Hippocampus—R. Thalamus Raw, $r = 0.31$, $p_b = 4 \times 10^{-5}$	8
	R. Hippocampus—R. Superior frontal cortex Augmented, $r = 0.32$, $p_b = 3 \times 10^{-7}$	95
MoCA Delayed recall—no cue	R. Hippocampus—R. Thalamus Raw, $r = 0.31$, $p_b = 3 \times 10^{-5}$	3
	R. Hippocampus—L. Superior frontal cortex Augmented, $r = 0.26$, $p_b = 0.006$	4
Free and Cued Selective Reminding Test Trial 1 Free Recall	R. Hippocampus—R. Precentral cortex Raw, $r = 0.33$, $p_b = 8 \times 10^{-12}$	30
	R. Hippocampus—L. Thalamus Augmented, $r = 0.34$, $p_b = 2 \times 10^{-13}$	158
Free and Cued Selective Reminding Test Trial 1 Cued Recall	R. Hippocampus—R. Precentral cortex Raw, $r = -0.25$, $p_b = 0.0002$	2
	R. Hippocampus—R. Precentral cortex Augmented, $r = -0.21$, $p_b = 0.03$	3
Free and Cued Selective Reminding Test Trial 2 Free Recall	L. Hippocampus—L. Ventral diencephalon Raw, $r = 0.32$, $p_b = 4 \times 10^{-10}$	38
	R. Hippocampus—L. Hippocampus Augmented, $r = 0.38$, $p_b = 10^{-18}$	350
Free and Cued Selective Reminding Test Trial 2 Cued Recall	R. Hippocampus—R. Precentral cortex Raw, $r = -0.28$, $p_b = 2 \times 10^{-6}$	16
	L. Hippocampus—R. Superior frontal cortex Augmented, $r = -0.3$, $p_b = 4 \times 10^{-10}$	94
Free and Cued Selective Reminding Test Trial 3 Free Recall	R. Hippocampus—R. Putamen Raw, $r = 0.31$, $p_b = 7 \times 10^{-10}$	41

(Continues)

TABLE 2 (Continued)

Non-MRI variable	Most correlated brain structural connection (type [raw/augmented], Pearson correlation, Bonferroni-corrected p-value)	# Sig. Conn
	R. Hippocampus—R. Superior frontal cortex Augmented, $r = 0.39$, $p_b = 5 \times 10^{-21}$	687
Free and Cued Selective Reminding Test Trial 3 Cued Recall	R. Hippocampus—R. Precentral cortex Raw, $r = -0.28$, $p_b = 10^{-6}$	26
	R. Hippocampus—R. Superior frontal cortex Augmented, $r = -0.34$, $p_b = 6 \times 10^{-14}$	233
Free and Cued Selective Reminding Test free summary score	R. Hippocampus—R. Precentral cortex Raw, $r = 0.35$, $p_b = 4 \times 10^{-13}$	44
	R. Hippocampus—R. Superior frontal cortex Augmented, $r = 0.39$, $p_b = 7 \times 10^{-21}$	541
Free and Cued Selective Reminding Test total score	R. Hippocampus—R. Ventral diencephalon Raw, $r = 0.23$, $p_b = 0.02$	2
	R. Hippocampus—L. Thalamus Augmented, $r = 0.27$, $p_b = 10^{-6}$	167
Clinician diagnosis: normal cognition	R. Hippocampus—R. Amygdala Raw, $r = 0.32$, $p_b = 2 \times 10^{-11}$	69
	R. Hippocampus—R. Superior frontal cortex Augmented, $r = 0.41$, $p_b = 3 \times 10^{-24}$	1648
Clinician diagnosis: Alzheimer's disease	R. Hippocampus—R. Fusiform cortex Raw, $r = -0.3$, $p_b = 6 \times 10^{-6}$	19
	L. Hippocampus—R. Lingual cortex Augmented, $r = -0.35$, $p_b = 2 \times 10^{-10}$	308
Amyloid burden (Centiloid scale) mean cortical binding potential	L. Parahippocampal cortex—L. Ventral diencephalon Raw, $r = -0.27$, $p_b = 0.007$	2
	L. Hippocampus—R. Superior temporal cortex Augmented, $r = -0.31$, $p_b = 2 \times 10^{-5}$	46
Amyloid burden (Centiloid scale) mean cortical standardized uptake value ratio (SUVR)	L. Parahippocampal cortex—L. Ventral diencephalon Raw, $r = -0.26$, $p_b = 0.0003$	8
	L. Hippocampus—R. Superior temporal cortex Augmented, $r = -0.31$, $p_b = 10^{-7}$	144
Amyloid burden (Centiloid scale) mean cortical binding potential (partial-volume corrected)	L. Parahippocampal cortex—L. Ventral diencephalon Raw, $r = -0.28$, $p_b = 0.001$	4
	L. Hippocampus –R. Superior temporal cortex Augmented, $r = -0.34$, $p_b = 10^{-7}$	86
Amyloid burden (Centiloid scale) mean cortical standardized uptake value ratio (SUVR) (partial-volume corrected)	L. Parahippocampal cortex—L. Ventral diencephalon Raw, $r = -0.29$, $p_b = 5 \times 10^{-6}$	20
	L. Hippocampus—R. Superior temporal cortex Augmented, $r = -0.35$, $p_b = 6 \times 10^{-12}$	608

Abbreviations: ADRC, Alzheimer's Disease Research Center; CDR, Clinical Dementia Rating; CT, computerized tomography; MoCA, Montreal cognitive assessment; MINT, Multilingual Naming Test; MRI, magnetic resonance imaging; OASIS-3, Open Access Series of Imaging Studies; PET, positron emission tomography; Sig.Conn, significant correlation; WAIS, Wechsler Adult Intelligence Scale; WMS, Wechsler Memory Scale.

TABLE 3 Significant correlations of non-MRI variables with brain connectivity in PREVENT-AD.

Non-MRI variable	Most correlated brain structural connection (type [raw/augmented], Pearson correlation, Bonferroni-corrected p-value)	# Sig.Conn
Age	R. Hippocampus—R. Thalamus Raw, $r = -0.33$, $p_b = 0.002$	2
	L. Hippocampus—R. Thalamus Augmented, $r = -0.33$, $p_b = 0.001$	13
Age of mother at AD-like dementia onset	R. Ventral diencephalon—L. Banks of superior temporal sulcus Raw, $r = -0.36$, $p_b = 0.006$	1
Tau phosphorylated at Thr181 (P-tau) concentration in CSF	R. Caudate—L. Caudal middle frontal cortex Raw, $r = 0.45$, $p_b = 0.04$	1

Abbreviations: AD, Alzheimer's disease; CSF, cerebrospinal fluid; MRI, magnetic resonance imaging; PREVENT-AD, Pre-symptomatic Evaluation of Experimental or Novel Treatments for Alzheimer's Disease; Sig.Conn, significant correlation.

TABLE 4 Significant correlations of non-MRI variables with brain connectivity in HCP.

Non-MRI variable	Most correlated brain structural connection (type [raw/augmented], Pearson correlation, Bonferroni-corrected p-value)	# Sig.Conn
Sex	Brainstem—L. Paracentral cortex Raw, $r = -0.24$ (with the male sex), $p_b = 0.007$	2
Height	R. Parahippocampal cortex—L. Paracentral cortex Augmented, $r = -0.22$, $p_b = 0.0497$	1
Weight	R. Ventral diencephalon—L. Ventral diencephalon Raw, $r = -0.24$, $p_b = 0.008$	5

Abbreviations: HCP, Human Connectome Project; MRI, magnetic resonance imaging.

some of which might have been spurious due to possible correlation with ICV, for example, strength, sex, alcohol consumption, and posture. Correlation of brain connectivity with sex,[45,46] in particular, remained inconclusive, given that it disappeared in PREVENT-AD (and was weakened in OASIS-3 and HCP) after ICV adjustment, as is typically seen in neuroimaging studies,[47,48] and appeared in ADNI-2 only after ICV adjustment, which could be a sign of an introduced (previously absent) ICV bias[49] (especially as the direction of the relationship in ADNI-2 was opposite to that in OASIS-3).

Differences in scanner hardware, population characteristics, and protocols across databases introduce database-dependent effects on both the acquired images and the measured variables (see the figures). Such effects could create large variances in both measured brain connectivity and non-MRI variables (those common in multiple databases) if databases were combined in a single heterogeneous correlation analysis. To prevent the natural population-level variances—which lead to true correlations—from being overshadowed by heterogeneity variances due to multi-database combination, we decided to analyze the databases independently and then compare the findings. Although data harmonization[50] in a combined database setting could reduce the heterogeneity to some extent, it would take away the benefit of replicability assessment across databases. Note that even within a single database, data may come from various sites; however, the within-database site effect is expected to be smaller, as all sites supposedly

often follow the same database-wide protocol. Data harmonization could nevertheless increase the statistical power when analyzing a multi-site database.

To correct for multiple comparisons, we took the conservative Bonferroni approach to avoid false-positive relationships with brain connectivity (reducing type I errors). Strong interdependencies both between brain connections and between non-MRI variables can nevertheless be exploited to design a complex but more forgiving correction scheme in order to avoid false negatives and missing existing relationships (reducing type II errors).

5 | CONCLUSIONS

We conducted a retrospective exploratory study to examine the associations between brain structural connectivity and non-MRI variables, using data from four (including three AD-related) public dMRI databases. Unlike hypothesis-driven research, where conjectured relationships between specific variables are tested, we calculated the correlation between all brain connections and non-MRI variables in our dataset without prior assumption, while stringently correcting for multiple comparisons, with the aim of discovering connectomic relationships. Replication of our findings in other databases (such as ADNI-3) and with other connectivity quantification methods and
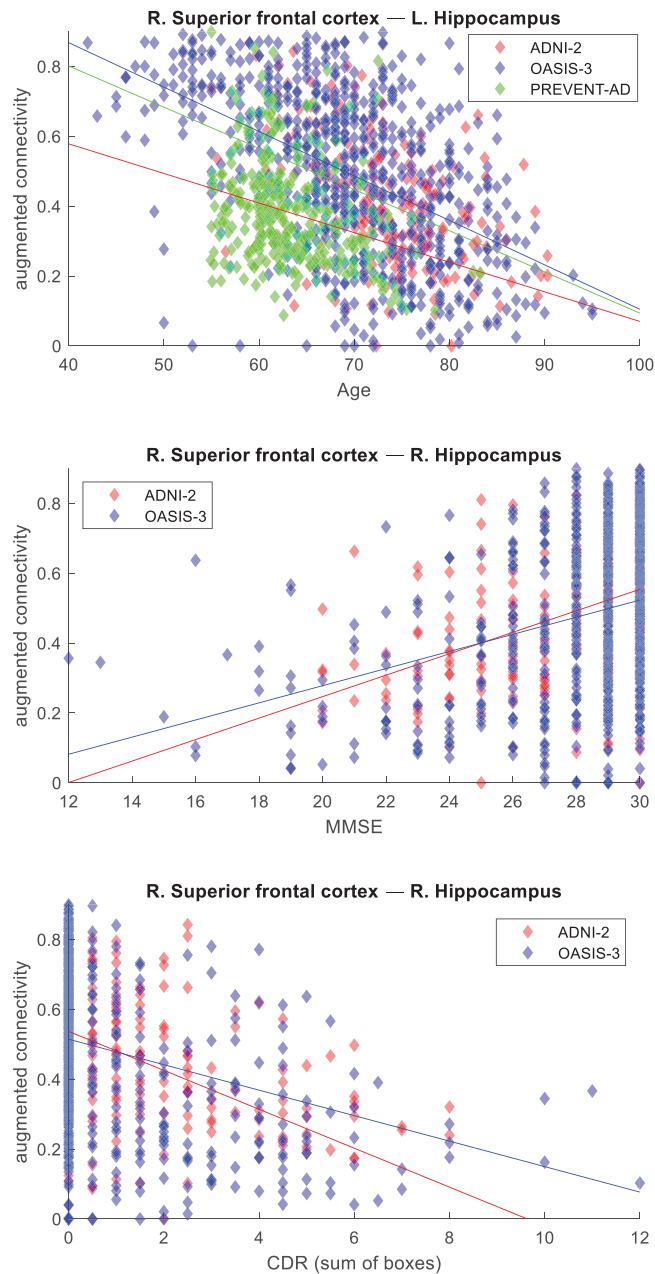
FIGURE 2 Augmented connectivity of the brain connection most significantly correlated with age (top), MMSE (middle), and CDR (bottom) consistently across databases. ADNI-2, Alzheimer's Disease Neuroimaging Initiative; CDR, Clinical Dementia Rating; MMSE, Mini-Mental State Examination; OASIS-3, Open Access Series of Imaging Studies; PREVENT-AD, Pre-symptomatic Evaluation of Experimental or Novel Treatments for Alzheimer's Disease.

conducting our study with harmonized dMRI data are subjects of future research.

16 NIH Institutes and Centers that support the NIH Blueprint for Neuroscience Research; and by the McDonnell Center for Systems Neuroscience at Washington University.

CONFLICT OF INTEREST STATEMENT

B. Fischl has a financial interest in CorticoMetrics, a company whose medical pursuits focus on brain imaging and measurement technologies. His interests were reviewed and are managed by Massachusetts General Hospital and Mass General Brigham in accordance with their conflict-of-interest policies. I. Aganj, J. Mora, and A. Frau-Pascual have nothing to disclose. Author disclosures are available in the supporting information.

CONSENT STATEMENT

Given our secondary and retrospective use of publicly available anonymized data, consent from subjects was not necessary.

ORCID

Iman Aganj https://orcid.org/0000-0002-4673-1293

REFERENCES

1. Tijms BM, Wink AM, de Haan W, et al. Alzheimer's disease: connecting findings from graph theoretical studies of brain networks. *Neurobiol Aging*. 2013;34:2023-2036.
2. Filippi M, Agosta F. Structural and functional network connectivity breakdown in Alzheimer's disease studied with magnetic resonance imaging techniques. *J Alzheimer's Dis*. 2011;24:455-474.
3. de LaCoste M-C, White CL. The role of cortical connectivity in Alzheimer's disease pathogenesis: a review and model system. *Neurobiol Aging*. 1993;14:1-16.
4. Sporns O. The human connectome: a complex network. *Ann NY Acad Sci*. 2011;1224:109-125.
5. Hafkemeijer A, van der Grond J, Rombouts SARB. Imaging the default mode network in aging and dementia. *Biochim Biophys Acta*. 2012;1822:431-441.
6. Greicius MD, Srivastava G, Reiss AL, Menon V. Default-mode network activity distinguishes Alzheimer's disease from healthy aging: evidence from functional MRI. *Proc Natl Acad Sci USA*. 2004;101:4637-4642.
7. Lee WJ, Han CE, Aganj I, Seo SW, Seong J-K. Distinct patterns of Rich Club Organization in Alzheimer's disease and subcortical vascular dementia: a white matter network study. *J Alzheimer's Dis*. 2018;63:977-987.
8. Rose SE, Chen F, Chalk JB, et al. Loss of connectivity in Alzheimer's disease: an evaluation of white matter tract integrity with colour coded MR diffusion tensor imaging. *J Neurol Neurosurg Psychiatry*. 2000;69:528-530.
9. Chhatwal JP, Schultz AP, Johnson KA, et al. Preferential degradation of cognitive networks differentiates Alzheimer's disease from ageing. *Brain*. 2018;141:1486-1500.
10. Rubinov M, Sporns O. Complex network measures of brain connectivity: uses and interpretations. *Neuroimage*. 2010;52:1059-1069.
11. Reijmer YD, Leemans A, Caeyenberghs K, et al. Disruption of cerebral networks and cognitive impairment in Alzheimer disease. *Neurology*. 2013;80:1370-1377.
12. Jbabdi S, Johansen-Berg H. Tractography: where do we go from here? *Brain Connect*. 2011;1:169-183.
13. Aganj I, Lenglet C, Jahanshad N, et al. A Hough transform global probabilistic approach to multiple-subject diffusion MRI tractography. *Med Image Anal*. 2011;15:414-425.

14. Honey CJ, Sporns O, Cammoun L, et al. Predicting human resting-state functional connectivity from structural connectivity. *Proc Natl Acad Sci*. 2009;106:2035-2040.
15. Deligianni F, Robinson E, Beckmann CF, Sharp D, Edwards AD, Rueckert D. Inference of functional connectivity from direct and indirect structural brain connections. Biomedical Imaging: from Nano to Macro, 2011 IEEE International Symposium on, 2011. p. 849-852.
16. Aganj I, Prasad G, Srinivasan P, Yendiki A, Thompson PM, Fischl B. Structural brain network augmentation via Kirchhoff's laws. Annual Meeting of the International Society for Magnetic Resonance in Medicine, 2014.
17. Frau-Pascual A, Fogarty M, Fischl B, Yendiki A, Aganj I. Quantification of structural brain connectivity via a conductance model. *Neuroimage*. 2019;189:485-496.
18. Frau-Pascual A, Augustinack J, Varadarajan D, et al. Conductance-based structural brain connectivity in aging and dementia. *Brain Connect*. 2021;11:566-583.
19. Wyman BT, Harvey DJ, Crawford K, et al. Standardization of analysis sets for reporting results from ADNI MRI data. *Alzheimers Dement*. 2013;9:332-337.
20. LaMontagne PJ, Benzinger TL, Morris JC, et al. OASIS-3: longitudinal neuroimaging, clinical, and cognitive dataset for normal aging and Alzheimer disease. *medRxiv*. 2019:2019.12.13. 19014902.
21. Tremblay-Mercier J, Madjar C, Das S, et al. Open science datasets from PREVENT-AD, a longitudinal cohort of pre-symptomatic Alzheimer's disease. *NeuroImage: Clinical*. 2021;31:102733.
22. Van Essen DC, Smith SM, Barch DM, Behrens TEJ, Yacoub E, Ugurbil K. The WU-Minn Human Connectome Project: an overview. *Neuroimage*. 2013;80:62-79.
23. Fischl B. FreeSurfer. *Neuroimage*. 2012;62:774-781.
24. Reuter M, Schmansky NJ, Rosas HD, Fischl B. Within-subject template estimation for unbiased longitudinal image analysis. *Neuroimage*. 2012;61:1402-1418.
25. Jenkinson M, Beckmann CF, Behrens TEJ, Woolrich MW, Smith SM. FSL. *Neuroimage*. 2012;62:782-790.
26. Greve DN, Fischl B. Accurate and robust brain image alignment using boundary-based registration. *Neuroimage*. 2009;48:63-72.
27. Aganj I, Lenglet C, Sapiro G, Yacoub E, Ugurbil K, Harel N. Reconstruction of the orientation distribution function in single- and multiple-shell q-ball imaging within constant solid angle. *Magn Reson Med*. 2010;64:554-566.
28. Greicius MD, Supekar K, Menon V, Dougherty RF. Resting-state functional connectivity reflects structural connectivity in the default mode network. *Cereb Cortex*. 2008;19:72-78.
29. Adachi Y, Osada T, Sporns O, et al. Functional connectivity between anatomically unconnected areas is shaped by collective network-level effects in the macaque cortex. *Cereb Cortex*. 2011;22:1586-1592.
30. Damoiseaux J, Greicius M. Greater than the sum of its parts: a review of studies combining structural connectivity and resting-state functional connectivity. *Brain Struct Funct*. 2009;213:525-533.
31. Huang H, Ding M. Linking functional connectivity and structural connectivity quantitatively: a comparison of methods. *Brain Connect*. 2016;6:99-108.
32. Koch MA, Norris DG. Hund-Georgiadis M. An investigation of functional and anatomical connectivity using magnetic resonance imaging. *Neuroimage*. 2002;16:241-250.
33. Skudlarski P, Jagannathan K, Calhoun VD, Hampson M, Skudlarska BA, Pearlson G. Measuring brain connectivity: diffusion tensor imaging validates resting state temporal correlations. *Neuroimage*. 2008;43:554-561.
34. van den Heuvel MP, Mandl RCW, Kahn RS, Hulshoff Pol HE. Functionally linked resting-state networks reflect the underlying structural connectivity architecture of the human brain. *Hum Brain Mapp*. 2009;30:3127-3141.

35. Chung MK, Hanson JL, Adluru N, Alexander AL, Davidson RJ, Pollak SD. Integrative structural brain network analysis in diffusion tensor imaging. *Brain Connect*. 2017;7:331-346.

36. Rousselet G, Pernet C. Improving standards in brain-behavior correlation analyses. *Front Hum Neurosci*. 2012;6.

37. Aganj I, Frau-Pascual A, Iglesias JE, et al. Compensatory brain connection discovery in Alzheimer's disease. 2020 IEEE 17th International Symposium on Biomedical Imaging (ISBI), 2020. p. 283-287.

38. Fortea J, Sala-Llonch R, Bartrés-Faz D, et al. Increased cortical thickness and caudate volume precede atrophy in PSEN1 mutation carriers. *J Alzheimer's Dis*. 2010;22:909-922.

39. Ryan NS, Keihaninejad S, Shakespeare TJ, et al. Magnetic resonance imaging evidence for presymptomatic change in thalamus and caudate in familial Alzheimer's disease. *Brain*. 2013;136:1399-1414.

40. Stern Y. Cognitive reserve and Alzheimer disease. *Alzheimer Dis Assoc Disord*. 2006;20:S69-S74.

41. Douaud G, Jbabdi S, Behrens TEJ, et al. DTI measures in crossing-fibre areas: increased diffusion anisotropy reveals early white matter alteration in MCI and mild Alzheimer's disease. *Neuroimage*. 2011;55:880-890.

42. Kim WH, Adluru N, Chung MK, et al. Multi-resolution statistical analysis of brain connectivity graphs in preclinical Alzheimer's disease. *Neuroimage*. 2015;118:103-117.

43. Grill JD, Kwon J, Teylan MA, et al. Retention of Alzheimer disease research participants. *Alzheimer Dis Assoc Disord*. 2019;33:299-306.

44. Lo RY, Jagust WJ. Predicting missing biomarker data in a longitudinal study of Alzheimer disease. *Neurology*. 2012;78:1376-1382.

45. Jahanshad N, Aganj I, Lenglet C, et al. Sex differences in the human connectome: 4-Tesla high angular resolution diffusion imaging (HARDI) tractography in 234 young adult twins. Biomedical Imaging: from Nano to Macro, 2011 IEEE International Symposium on, 2011. p. 939-943.

46. Kazi A, Mora J, Fischl B, Dalca AV, Aganj I. Multi-head graph convolutional network for structural connectome classification. *Proc 5th MICCAI Workshop on Graphs in Biomedical Image Analysis*. 2023:1-10.

47. Leonard CM, Towler S, Welcome S, et al. Size matters: cerebral volume influences sex differences in neuroanatomy. *Cereb Cortex*. 2008;18:2920-2931.

48. Choi CH, Lee JM, Koo BB, et al. Sex differences in the temporal lobe white matter and the corpus callosum: a diffusion tensor tractography study. *Neuroreport*. 2010;21:73-77.

49. Dhamala E, Ooi LQR, Chen J, et al. Proportional intracranial volume correction differentially biases behavioral predictions across neuroanatomical features, sexes, and development. *Neuroimage*. 2022;260:119485.

50. Ning L, Bonet-Carne E, Grussu F, et al. Cross-scanner and cross-protocol multi-shell diffusion MRI data harmonization: algorithms and results. *Neuroimage*. 2020;221:117128.

SUPPORTING INFORMATION

Additional supporting information can be found online in the Supporting Information section at the end of this article.

APPENDIX
COLLABORATORS

Data used in the preparation of this article were obtained from the Alzheimer's Disease Neuroimaging Initiative (ADNI) database (adni.loni.usc.edu). As such, the investigators within the ADNI contributed to the design and implementation of ADNI and/or provided data but did not participate in the analysis or writing of this report. A complete listing of ADNI investigators can be found at http://adni.loni.usc.edu/wp-content/uploads/how_to_apply/ADNI_Acknowledgement_List.pdf.